

Large-scale measurements using robotic volumetric LPT with Shake-the-Box inside a vehicle cabin: Influence of different fan speeds on the flow topology

T. Gericke^{1,*} J. C. Londono Alfaro¹ S. Hüttig¹

¹: Volkswagen AG, Wolfsburg

* Correspondent author: timo.gericke@volkswagen.de

Keywords: PTV, Shake-the-Box, Flow topology, Vehicle cabin

ABSTRACT

In this work, the flow topology inside a passenger car cabin for different fan speeds of the heat, ventilation and air conditioning (HVAC) system is investigated using robotic volumetric Lagrangian Particle Tracking (LPT). The coaxial volumetric velocimeter (CVV), also called MiniShaker, in combination with a robotic arm enables the measurement of the complete passenger's side. In total 37 CVV perspectives (sub-volumes) were measured. At each position 3000 double frame images were recorded. The interior was painted black and the mannequin was wrapped with black aluminum foil in order to keep reflections at a low level. Experimental results for three different fan speeds using helium-filled soap bubbles (HFSB) as tracers and Shake-the-Box (StB) algorithm for the three-dimensional LPT data analyses show that the flow topology changes significantly with increasing fan speeds. At higher fan speeds the flow fields show the highest complexity with four vortices.

1. Introduction

The heat, ventilation and air conditioning (HVAC) system is one of the largest secondary consumer in the car. Therefore, an efficient system can reduce the energy consumption and extend the driving range of electric vehicles which is one of the major goals for the automotive industry. Environmental air is heated or cooled in the HVAC system and directed through a system of ducts and outlets with grid vanes into the car cabin at various locations (e.g. driver's seat left and right, passenger seat left and right, etc.). New energy-saving designs require a deep understanding of the flow fields inside the system, at the vent outlets and jet stream areas. The flow mainly depends on the geometry of the ducts, the interior design, the shape of the outlets, the ambient conditions and the settings of the HVAC system.

Measurement techniques like Particle Image Velocimetry (PIV) and Particle Tracking Velocimetry (PTV) are promising techniques to deeply understand such flow fields [Huera-Huarte et al., 2014, Lee et al., 2011, Bertone et al., 2022, Ullrich et al., 2020], as well as in passenger aircraft cabins

[Elmaghraby et al., 2018]. Robotic volumetric PTV has the advantage of measuring a large volume of the flow compared to thin planes of large-scale PIV. This is achieved by the superposition of a multitude of observation domains (sub-volumes) from different acquisition perspectives. This can only be achieved by a measurement system controlled by means of a robotic arm that does not require calibration after repositioning of the system. Schneiders et al. (2018) introduced a compact coaxial volumetric velocimeter (CVV) also called MiniShaker (LaVision GmbH). The MiniShaker Aero MP is a multi-camera system with four cameras and laser expanding optics ideal for Shake-The-Box, double-pulse volumetric PTV and tomographic PIV.

In order to deepen the understanding of HVAC related flow fields, measurements using robotic volumetric LPT together with HFSB as tracers and a StB algorithm were carried out. An ID.4 was chosen as a test case for the measurements. The robotic arm together with the CVV was installed inside the car, whereas all other equipment was installed in the trunk or outside the wind tunnel test section. In total the flow fields for three different fan speeds were investigated.

2. Experimental Setup

Measurements were conducted at the closed loop wind tunnel facility of Volkswagen. The atmospheric wind tunnel has a nozzle exit section of 12 m². With a 2 MW electric motor free-stream velocities ranging from 5 to 70 m/s are possible. The test-section is 10 m long and 9.5 m wide. Turbulence intensity of the free stream is $\leq 0.4\%$ and the flow angularity ≤ 0.4 Grad. Free stream velocity was set to 14 m/s. The full-scaled car cabin of an ID.4 was used as an experimental test case. Air supply inside the cabin was accomplished via four front air vents (Fig. 2) and one central rear air vent. Front air vents are on the drivers and passenger door side as well as in the center. All other air vents (e.g. footwell etc.) were temporarily closed throughout the measurements. Grid vanes of the vents were set to a neutral position.

Temperature in the cabin was set to 20°C. All interior parts that are not originally black matt were painted with a black matt color or laminated with a black matt foil. The mannequin (originally white) was wrapped by a black matt aluminum foil (see Fig. 1). In total three different fan speeds (55%, 75% and 100%) of the HVAC system were investigated.

For the acquisitions of the recordings the CVV probe MiniShaker Aero MP (Fig. 1) from LaVision was used. It exhibits four CMOS-Cameras with a frame rate of 100 Hz at full resolution of 1920 x 1280 pixels with macro planar lenses (f -number = 4, $f\#$ = 12 mm) and a pixel pitch Δp_x of 4.8 μm . The focal point of the cameras is set at 440 mm from the center of the front cap. In addition, the CVV incorporates a spherical lens for the volumetric beam expansion. Illumination is provided by a Litron NanoPIV Nd:YAG laser with an output energy of 50 mJ per pulse at a wavelength of

532 nm and a frequency of 100 Hz. Laser light is transmitted with an optical fiber towards the CVV's head. The measurable volume is bound within the region where the camera views overlap in lateral and vertical direction. At a measurement distance of $z = 260$ mm, the FOV attains 220×130 mm² which extends to 450×350 mm² at $z = 670$ mm in the MiniShaker coordinate system. Synchronization between the laser and the cameras is assured by a PTU X from LaVision.

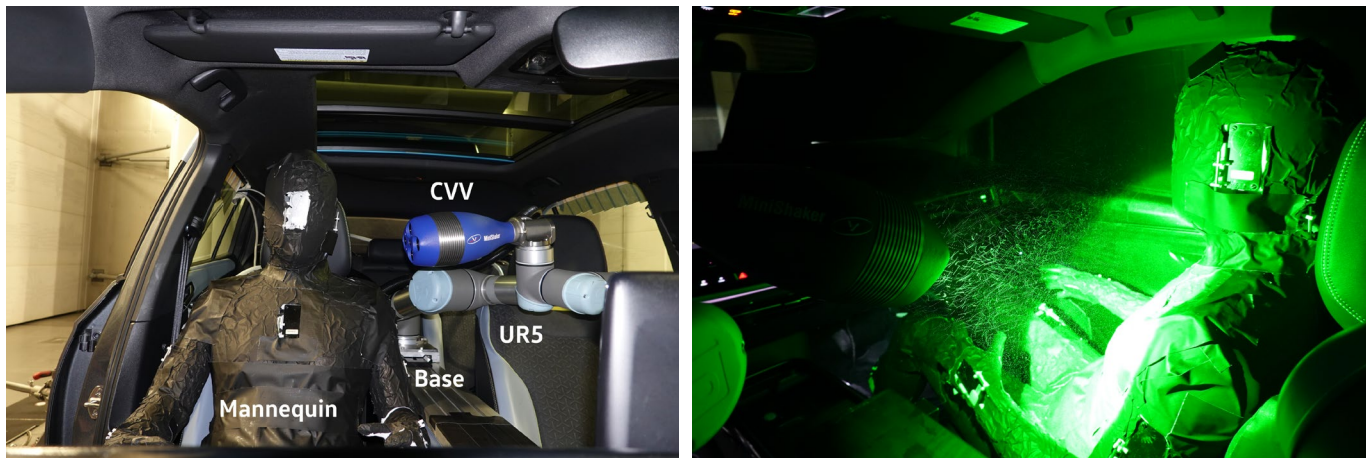


Figure. 1 Photograph of the mannequin on the passenger side together with the CVV (left). Particle visualization around the mannequin (right).

The CVV heads position and orientation is controlled by a robotic arm UR5 from Universal Robots (Jux et al. 2018) with six degrees of freedom (3 rotation and 3 translation axes), similar to the movement range of a human arm. Position repeatability is stated by the manufacturer as ± 0.1 mm (Universal Robots 2014). Maximum reach of the UR5 is 850 mm in radius around the robot base. In order to install the robotic arm in the car cabin a flat aluminum construction profile (item) is installed in the center line of the car (see Fig. 1). Raw particle images are gathered from a total of 37 positions (sub-volumes) covering most of the passenger's front seat (Fig.2). Sub-volumes are recorded at three different z-positions (Fig. 2) and at two different y-positions. At each robot-position 3000 double-frame images are recorded at a recording rate of 100 Hz.

Helium-filled soap bubbles were used as tracer particles with a mean size of $300 \mu\text{m}$. A HFSB generator (Fig. 3) from LaVision was used to generate the seeding particles. The system consists of a fluid supply unit (FSU) and two single nozzles (Fig. 3). Each nozzle produces 40.000 soap bubbles per second. In total 0.08×10^6 tracers per second are produced and distributed across the cabin with a volume of 2.9 m^3 . The nozzles were placed inside the HVAC system so that an efficient seeding is assured, and no seeding accumulates on the surface of filters, heat exchangers, etc.

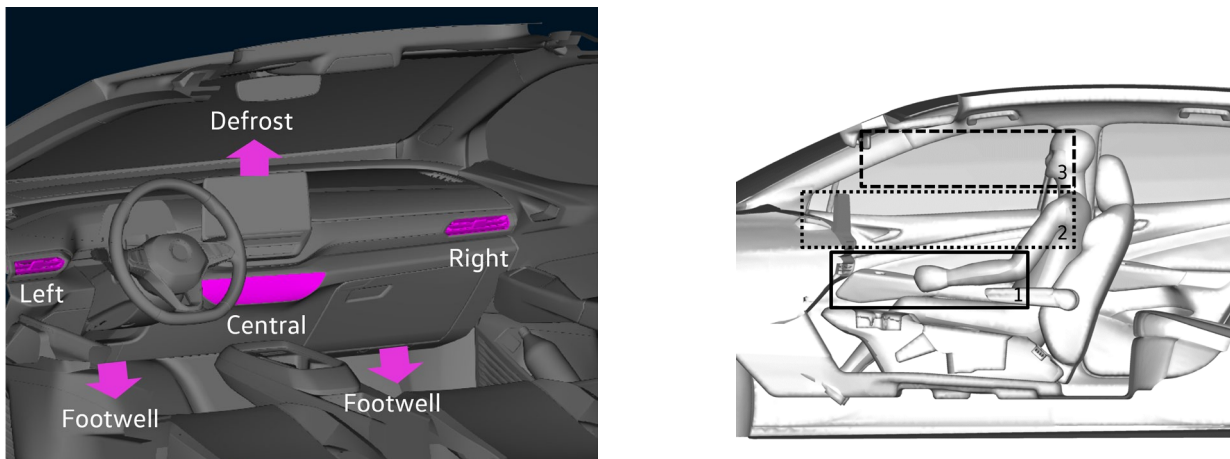


Figure. 2 Position of the front air vents in the full-scale car cabin. Not shown are the rear air vents, inlet and outlet (left). Different z-positions of the recorded sub-volumes (right).

A single-plane calibration plate (LaVision Type 286-39 SSSP) is used for the geometric calibration. The calibration plate consists of 42 dots with a center-to-center spacing of 40 mm and a dot diameter of 12 mm. Geometrical calibration was performed with five different views at $z = 440$ mm and the pinhole method. After the geometric calibration a volume self-calibration (Wieneke 2008) followed by the determination of the optical-transfer-function (OTF) (Schanz et al. 2012) is performed with the use of experimental data in DaVis 10.2.1.

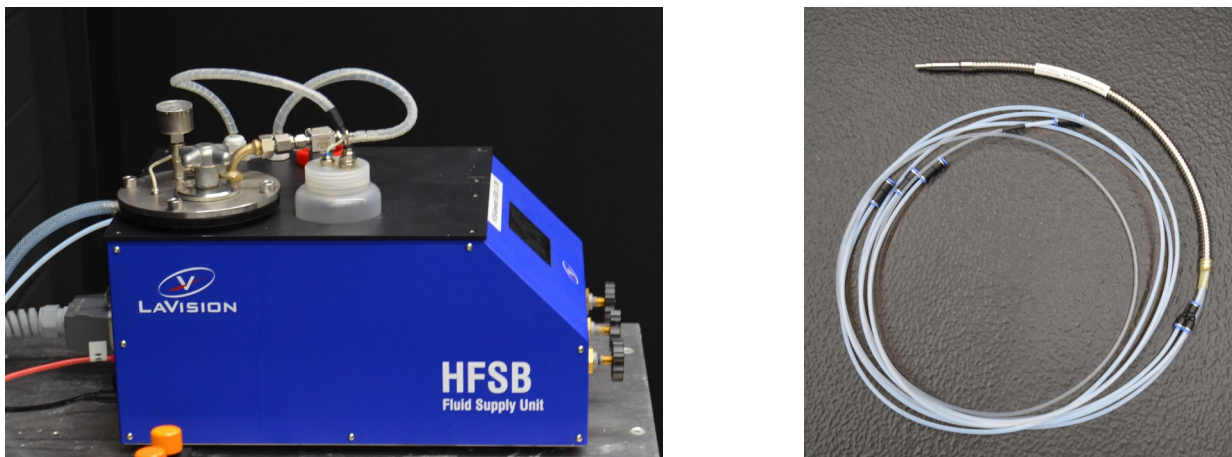


Figure. 3 HFSB generator (left). Single nozzle (right).

Raw particle images are pre-processed using the image pre-processing routine in DaVis 10. Main goal of pre-processing is the removal of background noise from the image in order to have clearly defined particle images with high contrast between the particles and the background. After the image pre-processing the particle images are analyzed with the Shake-The-Box algorithm implemented in DaVis. Approximately 2.100 particles are recorded in every image. Every sub-

volume contains approximately 850.000 tracks giving a total number of 31.450.000 tracks. After the particles are tracked, the sub-volumes are merged together (stitching). Afterwards the Lagrangian description of the velocity is converted into a Eulerian description through the binning process. The result is the mean velocity vector field. The interrogation window's size is 64 voxel with 75% overlap resulting in a grid size of 16 voxel (3.5 mm).

The dynamic spatial range DSR is defined as the ratio between the largest and the smallest measurable length scales (Adrian 1997). For the present setup the largest length scale is given by the length of the measured sub-volumes and the smallest length scale is given by the smallest used bin size.

$$\overline{DSR} = \frac{400 \text{ mm}}{14 \text{ mm}} = 28.6 \quad (1)$$

Another important parameter is the dynamic velocity range (DVR). The DVR is defined as the ratio between the maximum resolvable velocity and the minimum one (Adrian 1997). In the present case the ratio between the maximum measured velocity and the measurement uncertainty in the overlapping region of adjacent sub-volumes.

$$\overline{DVR} = \frac{0.3 \text{ m/s}}{0.001 \text{ m/s}} = 300 \quad (2)$$

3. Results

Figure 4-6 show the mean velocity fields from the Lagrangian description converted into a Eulerian description through the binning process at $y/H = 0.15$ (left), 0.30 (middle) and 0.38 (right) for the three different fan speeds of the HVAC system. Different fan speeds of 55%, 75% and 100% are arranged from top (Fig. 4) to bottom (Fig. 6). Gaps in the vector fields are a direct result of reflections inside the measurement volume. Clearly visible is the complex system of different large- and small-scale vortices rotating in clockwise and counter-clockwise direction. For a fan speed of 55% a large counter-clockwise vortex A dominates most of the measured flow field at $y/H = 0.15$ (Fig. 4, left) with the center of the vortex located between the dashboard and the mannequin. Portions of a second vortex B with clockwise rotation can be seen between the dashboard and the windshield. At $y/H = 0.30$ (Fig. 4, middle) the main vortex A moves closer to the ceiling towards the mannequin's face with the center of the vortex at the height of the neck. Moreover, streamlines show that air is entrained from the legroom towards the passenger seat

forming another vortex C which is not the case at $y/H = 0.15$. Here, streamlines show in the opposite direction. Flow injected from the passenger's vent ($y/H = 0.38$, Fig. 4, right) cause the aforementioned large counter-clockwise vortex A. Compared to $y/H = 0.30$ the center of the vortex is very similar. The highest streamwise velocity for this fan speed occurs behind the outlet and has a magnitude of 0.27 m/s.

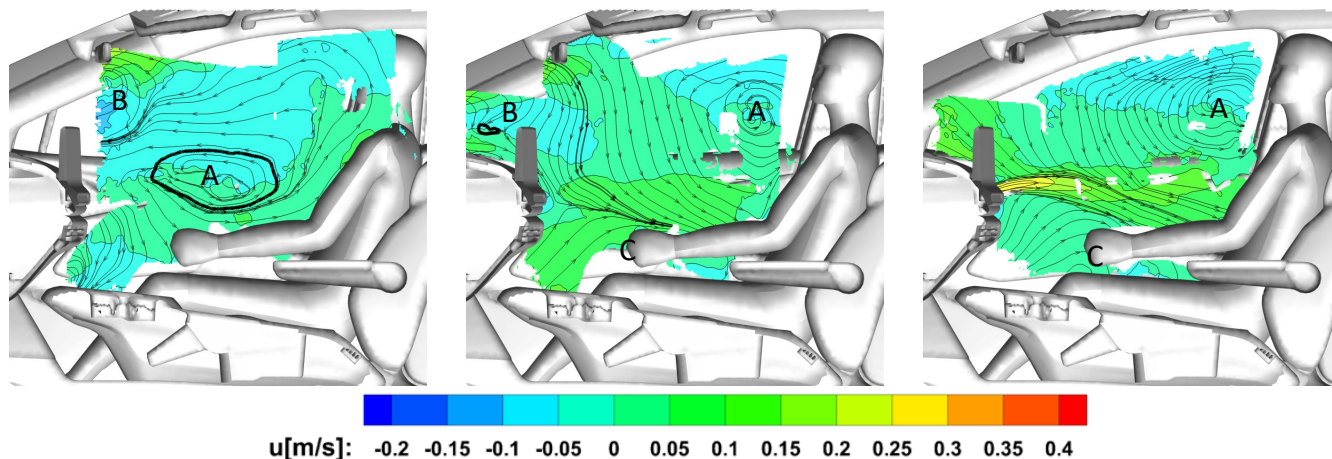


Figure. 4 Mean velocity field at $y/H = 0.15$ (left), 0.30 (middle) and 0.38 (right) for a fan speed of 55% color coded by the normalized streamwise velocity.

For a fan speed of 75% (Fig. 5) the center of the large counter-clockwise vortex A stays more or less at the height of the neck for all three planes. Overall the vortex seems to be smaller compared to the lower fan speed. The highest streamwise velocity occurs behind the outlet and has a magnitude of 0.38 m/s.

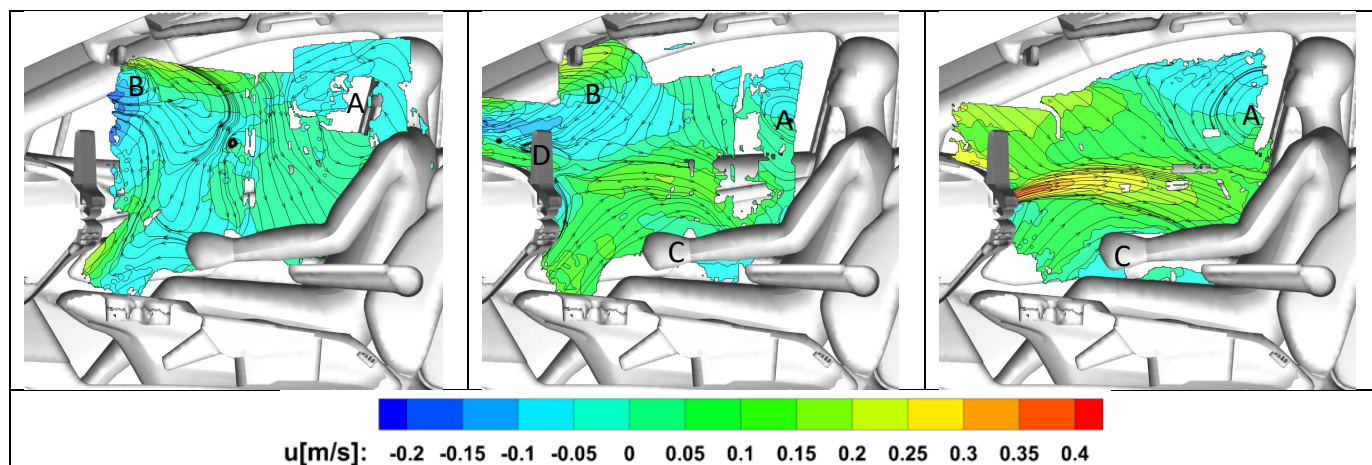


Figure. 5 Mean velocity field at $y/H = 0.15$ (left), 0.30 (middle) and 0.38 (right) for a fan speed of 75% color coded by the normalized streamwise velocity.

Compared to a fan speed of 55% the jet stream issued from the passenger vent elongates further into the car cabin which is most probably the reason for the observed smaller counter-clockwise vortex A. A second vortex B with clockwise rotation can be seen between the dashboard and the windshield similar to the lower fan speed. Also vortex C is there. At $y/H = 0.30$ (Fig. 5, middle) an additional counter-clockwise vortex D occurs above the femurs that is much smaller than A, B and C.

A fan speed of 100% (Fig. 6) shows a similar complex flow structure compared to a fan speed of 75%. Vortex C and D are significantly larger, whereas A and B are smaller. The increase of D and the changes for A, B and C are direct results of the jet stream issued from the passenger vent elongating much further into the car cabin. Streamwise velocity behind the outlet has a magnitude of the same order as the 75% case.

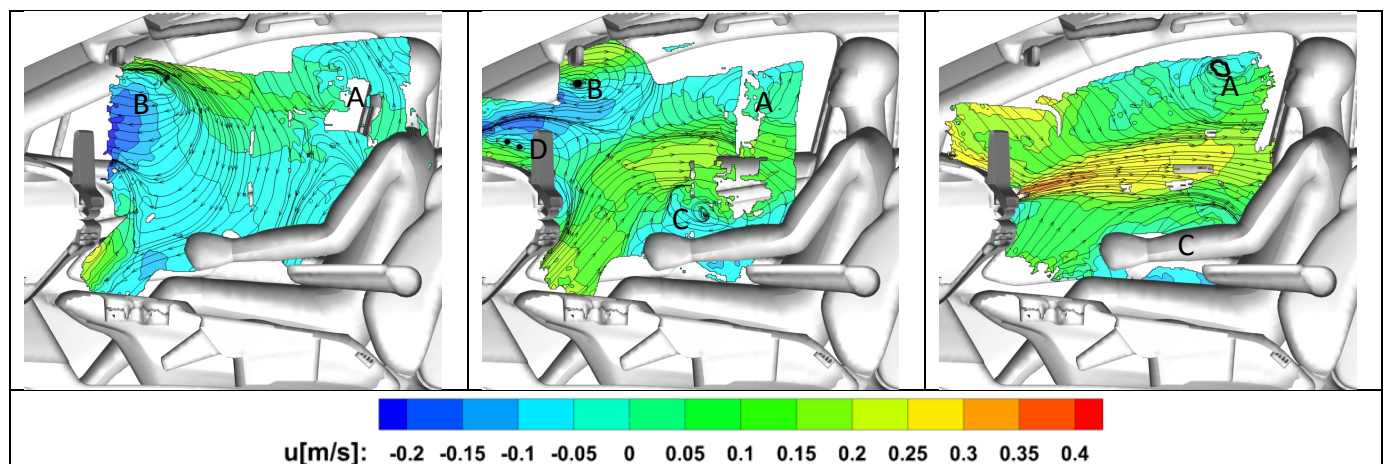


Figure. 6 Mean velocity field at $y/H = 0.15$ (left), 0.30 (middle) and 0.38 (right) for a fan speed of 100% color coded by the normalized streamwise velocity.

Figure 7 shows the isosurfaces of the velocity colored by $u = 0.2$ m/s for the three different fan speeds. Clearly visible is the entrainment of fluid from the dashboard for higher fan speeds.

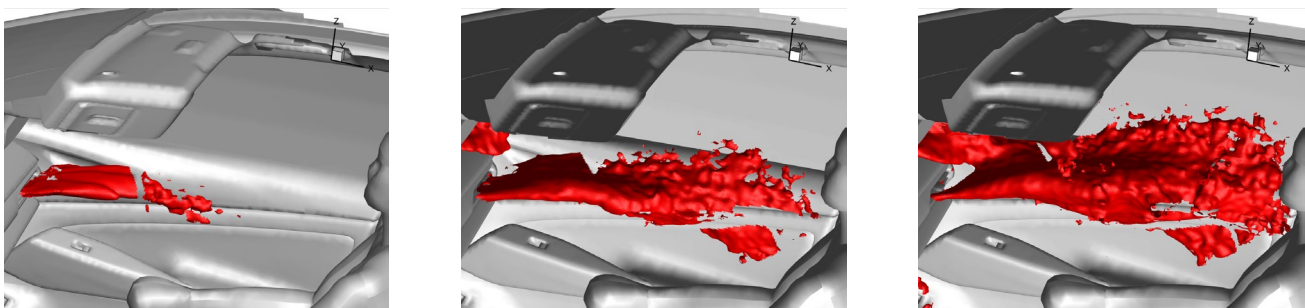


Figure. 7 Isosurface of the velocity colored by $u = 0.2$ m/s for a fan speed of 55% (left), 75% (middle) and 100% (right).

4. Conclusion

In this study, the flow topology inside a passenger car cabin for different fan speeds (55%, 75% and 100%) of the heat, ventilation and air conditioning (HVAC) system has been successfully investigated using robotic volumetric Lagrangian Particle Tracking (LPT). Data can be used as a benchmark for the validation of CFD.

Main advantage of the setup is the availability of flow field data in a volume compared to thin light sheets. Thus, the complexity of the flow can be analyzed in much more detail and therefore leading to a much better understanding of such complex flow fields.

At the highest fan speed the jet stream issued from the passenger vent extends far into the car cabin. Also, the flow fields at higher fan speeds show the maximum complexity in this investigation. In total four vortices with different sizes and both clockwise and counter-clockwise rotations are present.

In future measurement campaigns more sub-volumes should be recorded in order to avoid gaps in the vector fields due to reflections. A doubling of the number of sub-volumes is suggested for such an area of interest.

The results, opinions and conclusions expressed in this publication are not necessarily those of Volkswagen Aktiengesellschaft.

Acknowledgements

The authors would like to acknowledge the colleagues from LaVision for their support throughout the measurement campaign and the evaluation phase.

References

- Adrian, R. J. (1997) Dynamic ranges of velocity and spatial resolution of particle Image velocimetry. *Measurement Science and Technology*, 8(12):1393
- Bertone, M., Sciacchitano, A., Arpino, F.; Canale, C., Cortellessa, g., Grossi, L. & Moretti, L. (2022). Experimental characterization of the airflow within a car cabin. *39th Heat Transfer Conference, Journal of Physics: Conference Series*, 2509
- Elmaghraby, H. A., Chiang, Y. W. and Aliabadi, A. A. (2018). Ventilation strategies and air quality management in passenger aircraft cabins: A review of experimental approaches and numerical simulations. *Science and Technology for the Built Environment*, 24, 160-175
- Huera-Huarte, F. J., Cort, X. & Aramburu, E. (2014). DPIV measurements of the HVAC aerodynamics inside a passenger car. *SAE Technical Papers*
- Lee, J. P., Kim, H. K. & Lee, S. J. (2011). Large-scale PIV measurements of ventilation flow inside the passenger compartment of a real car. *Journal of Visualization*, 14, 321-329
- Schanz, D., Gesemann, S., Schröder, A., Wieneke, B. & Novara M. (2012). Non-uniform optical transfer functions in particle imaging: calibration and application to tomographic reconstruction. *Measurement Science and Technology*, 24(2):024009
- Schanz, D., Gesemann, S. & Schröder, A. (2016b). Shake-The-Box: Lagrangian particle tracking at high particle image densities. *Experiments in Fluids*, 57(5), 1-27
- Ullrich, S., Buder, R., Boughanmi, N., Friebe, C. & Wagner, C. (2020). Numerical study of the airflow distribution in a passenger car cabin validated with PIV. *21st STAB/DGLR Symposium, Darmstadt, New Results in Numerical and Experimental Fluid Mechanics XII*, pp. 457-467
- Wieneke, B. (2008). Volume self-calibration for 3D particle image velocimetry. *Experiments in Fluids*, 45(4), 549-556